Evolution of High-Temperature Superconductivity from a Low-T_c Phase Tuned by Carrier Concentration in FeSe Thin Flakes

B. Lei,[1] J. H. Cui,[1] Z. J. Xiang,[1] C. Shang,[1] N. Z. Wang,[1] G. J. Ye,[1] X. G. Luo,[1,4] T. Wu,[1,4] Z. Sun,[2,4] and X. H. Chen[1,3,4,*]

[1]*Hefei National Laboratory for Physical Science at Microscale and Department of Physics, and Key Laboratory of Strongly-coupled Quantum Matter Physics, Chinese Academy of Sciences, University of Science and Technology of China, Hefei, Anhui 230026, China*

[2]*National Synchrotron Radiation Laboratory, University of Science and Technology of China, Hefei, Anhui 230026, China*

[3]*High Magnetic Field Laboratory, Chinese Academy of Sciences, Hefei, Anhui 230031, China*

[4]*Collaborative Innovation Center of Advanced Microstructures, Nanjing University, Nanjing 210093, China*

(Received 19 October 2015; revised manuscript received 28 December 2015; published 18 February 2016)

We report the evolution of superconductivity in an FeSe thin flake with systematically regulated carrier concentrations by the liquid-gating technique. With electron doping tuned by the gate voltage, high-temperature superconductivity with an onset at 48 K can be achieved in an FeSe thin flake with T_c less than 10 K. This is the first time such high temperature superconductivity in FeSe is achieved without either an epitaxial interface or external pressure, and it definitely proves that the simple electron-doping process is able to induce high-temperature superconductivity with $T_c^{\rm onset}$ as high as 48 K in bulk FeSe. Intriguingly, our data also indicate that the superconductivity is suddenly changed from a low-T_c phase to a high-T_c phase with a Lifshitz transition at a certain carrier concentration. These results help to build a unified picture to understand the high-temperature superconductivity among all FeSe-derived superconductors and shed light on the further pursuit of a higher T_c in these materials.

DOI: 10.1103/PhysRevLett.116.077002

Heavily electron-doped FeSe-derived materials are currently the focus of research in the field of iron-based superconductors [1–5]. These materials, including $A_x\mathrm{Fe}_{2-y}\mathrm{Se}_2$ [1,2], $\mathrm{Li}_x(\mathrm{NH}_2)_y(\mathrm{NH}_3)_{1-y}\mathrm{Fe}_2\mathrm{Se}_2$ [3], (Li,Fe)OHFeSe [4], and a monolayer FeSe film on SrTiO_3 [5], share very similar electronic structures with only electron pockets near the Fermi level, and the absence of a nodal superconducting gap structure. These materials usually possess a high superconducting transition temperature T_c above 30 K, and their unique characteristics differ from the FeAs-based superconductors and challenge current theories on a unified picture of superconductivity in iron-based superconductors [6]. In particular, the monolayer FeSe thin film on a SrTiO_3 substrate has generated wide research interest because of its unexpected high-T_c superconductivity close to the boiling temperature of liquid nitrogen (77 K) [5,7–12]. On the other hand, bulk FeSe only exhibits superconductivity below 10 K [13]. Such a sharp contrast on T_c suggests that the artificial interface between FeSe and SrTiO_3 should be the key for such a dramatic enhancement of T_c [14–18]. Then, a coming question is what the working mechanism of the interface to enhance superconductivity is. Subsequent angle-resolved photoemission spectroscopy studies indicate that both electron doping and an electron-phonon interaction from the interface are crucial for the dramatic enhancement of T_c in the monolayer FeSe thin film [7–10,16,17]. Furthermore, a common electronic structure with a significant electron pocket around the M point in the Brillouin zone is found in FeSe-derived bulk high-T_c superconductors [such as (Li,Fe)OHFeSe, $\mathrm{Rb}_x\mathrm{Fe}_{2-y}\mathrm{Se}_2$] [19,20], which is similar to that of the FeSe thin film. These results suggest that just sufficient electron doping is already enough to enhance T_c from 8.5 K in the bulk to at least 40 K. A recent angle-resolved photoemission spectroscopy result on a potassium doped FeSe thin film has found that electron doping could induce superconductivity at 48 K. In order to fully understand the role of electron doping in an FeSe thin film, we use a liquid-gating technique to tune the electron density in an FeSe thin flake without an epitaxial interface. High-T_c superconductivity is successfully achieved with $T_c^{\rm onset}$ at 48 K by electron doping. Our result definitely proves that a simple electron-doping process is able to induce high-temperature superconductivity with $T_c^{\rm onset}$ reaching 48 K in FeSe without an interface.

An electric-double-layer transistor (EDLT) using ionic liquids as the gate dielectric is very efficient in tuning the carrier concentration as well as the Fermi energy [21,22]. When a gate voltage V_g is applied, the cations and anions in the ionic liquid move towards the sample or the gate electrode, depending on the voltage polarity, and form a Helmholtz electric double layer. This type of device works as a nanogap capacitor. The surface of the sample can be electrically modulated with the charge accumulation or depletion. To elucidate the nature of high temperature superconductivity in FeSe thin films [5,9], especially the superconductivity induced by carrier doping, we use FeSe thin flakes to fabricate an EDLT transport channel. Figure 1(a) depicts a schematic illustration of our FeSe-based EDLT. The ionic liquid DEME-TFSI was used as the

 © 2016 American Physical Society

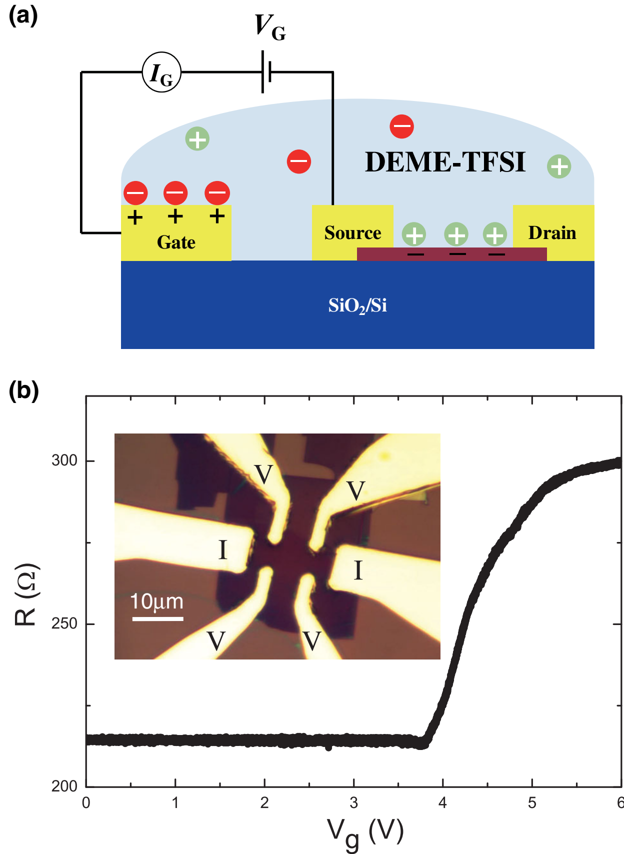

FIG. 1. (a) A schematic illustration of the FeSe thin flake EDLT device. The ionic liquid DEME-TFSI serves as the dielectric, covering the sample and gate electrodes. (b) Gate voltage dependence of the resistance of an FeSe thin flake with a typical thickness of about 10 nm during a continuously swept positive gate voltage at a scan rate of 1 mV s^{-1}. The inset shows an optical image of the EDLT device used in the present study.

dielectric, which has been found to show a large capacitance at low temperature [23]. The cations and anions are $DEME^+$ and $TFSI^-$, respectively. Detailed device preparation procedures are described in the Supplemental Material [24]. Using an EDLT, we systematically investigated the electrical transport properties of exfoliated single-crystalline FeSe thin flakes with typical thicknesses of about 10 nm. A continuously swept positive gate voltage with a scan rate of 1 mV s^{-1} was applied at 220 K, exactly the same conditions where the electric double layer has been found to form in previous works [21,22]. A typical R-V_g curve is shown in Fig. 1(b). The sheet resistance of the FeSe channel remains almost unchanged with V_g below 3.25 V then shows a small drop around $V_g \approx 3.75$ V, and then increases rapidly when V_g is ramped up to about 5.25 V, and eventually tends to saturate when V_g approaches 6 V. About a 40% enlargement in the sample resistance can be induced by $V_g = 6$ V.

The FeSe single crystals were grown by a flux method (for the characterization of the FeSe single crystals, see the Supplemental Material [24]). After the introduction of carriers to the FeSe channel surface at 220 K with the application of gate voltages, we measured the four-terminal sheet resistance R as a function of temperature T down to 2 K. The results are shown in Fig. 2. Before the gate voltage is applied, the FeSe flake shows an onset critical temperature $T_c^{\text{onset}} = 5.2$ K, slightly lower than that in the bulk crystal. Here, T_c^{onset} is defined as the intersection temperature between the linear extrapolation of the normal state and the superconducting transition, as illustrated in the inset of Fig. 2. With increasing V_g, T_c^{onset} slowly shifts to a high temperature, and reaches 7.5 K (close to T_c in a bulk FeSe single crystal) at $V_g = 4.0$ V. A further increase of V_g gives rise to a two-step superconducting transition in the sample. The low superconducting transition temperature nearly does not change, while the high one increases significantly from ~30 to above 40 K. Such a two-step transition should originate from the inhomogeneity of the carrier distribution. With $V_g > 5.0$ V, only the superconducting transition with T_c above 40 K can be observed and T_c^{onset} continuously increases with increasing V_g. Similar field-enhanced superconductivity has also been observed in other materials [35]. The high V_g also enhances the high temperature resistance and meanwhile suppresses the low temperature resistance of the sample, which leads to an increase of the residual resistance ratio value. At $V_g = 6$ V (the maximum voltage used in our experiment), the onset critical temperature T_c^{onset} increases to 45.3 K and zero resistance is realized at 30 K. It should be addressed that T_c at 6 V slightly depends on the sample and the highest T_c

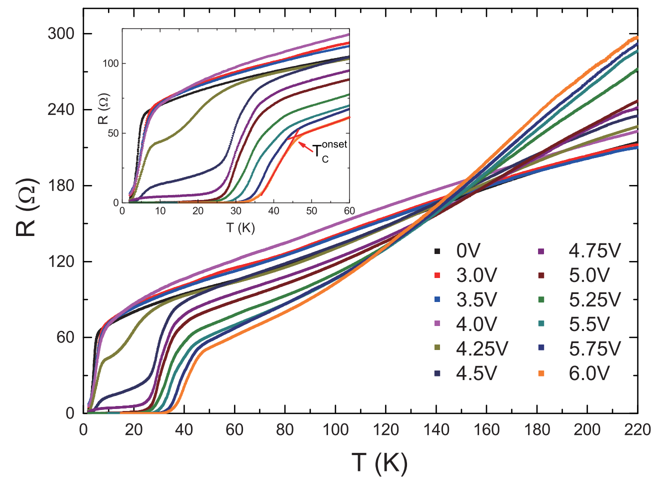

FIG. 2. Temperature dependence of the resistance for an FeSe thin flake at different V_g. The thickness of the flake is 10 nm, which is determined by atomic force microscopy (AFM). The sheet resistance was measured from 220 to 2 K with the gate bias ranging from 0 to 6 V. As the gate voltage is ramped up, T_c^{onset} is gradually enhanced. Eventually, the onset critical temperature T_c^{onset} of the sample increases up to 45.3 K and the sample reaches zero resistance at 30 K with $V_g = 6$ V. The inset is the magnified view of the region near the superconducting transition.

observed is 48.2 K (see the Supplemental Material, Fig. S3 [24]), which is higher than any other Fe-chalcogenide superconductors without an epitaxial interface. Upon applying $V_g > 6$ V, the samples became highly unstable and can be easily damaged, possibly owing to the electrochemical reaction above the threshold voltage. We mention that the evolution from the low-T_c phase to the high-T_c phase is largely reversible, as the low-T_c superconductivity could be restored by slowly sweeping V_g back to zero before reaching the threshold (see the Supplemental Material, Fig. S4 [24]).

To further reveal the evolution of the electronic properties in the gate voltage tuning process, we studied the Hall resistance R_{xy} of both bulk FeSe crystals and thin flakes under different V_g. The temperature dependence of the Hall coefficient R_H is summarized in Fig. 3(a). In bulk FeSe, $R_{xy}(B)$ curves exhibit a low-field nonlinearity at low temperature [Supplemental Material, Fig. S1(d) [24]], in

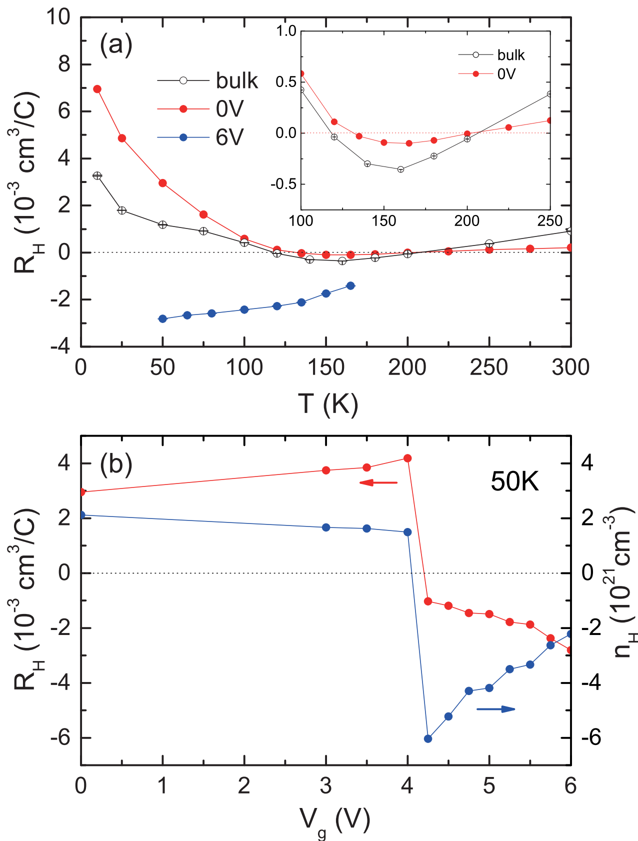

FIG. 3. (a) Temperature dependence of the Hall coefficient R_H. R_H was calculated from the linear fit of an R_{xy} vs B plot from −9 to 9 T. For the nonlinear $R_{xy}(B)$ curves, we extract R_H from the slope of the high-field quasilinear part. As V_g increases to 6 V, R_H changes sign from positive to negative at low temperature. The error bars are uncertainties of the linear fit. (b) Gate voltage dependence of the Hall coefficient R_H and the Hall number n_H at 50 K. At $V_g = 4.25$ V, R_H shows a sudden sign reversal, at which the dominant charge carrier changes from hole type to electron type.

agreement with previous reports [28,33]. For these curves, we extract R_H from the slope of the high-field quasilinear part since it is an indication of the effective carrier density [28]. The as-exfoliated FeSe flake shares a similar overall behavior of the temperature dependence of R_H with the bulk sample: the sign of R_H changes twice as the sample is cooled from room temperature to 2 K, and the sign of the low-temperature high-field Hall resistance is hole type. However, there are also some different features between the Hall resistance of the bulk crystals and the flakes. At $V_g = 0$ V, the low-field negative slope of $R_{xy}(B)$ in the low-temperature normal state of bulk FeSe is absent in the FeSe thin flakes, in which the value of R_H is also larger [Supplemental Material, Fig. S5(a) [24]]. Such observations indicate a downward shifted chemical potential E_F in the FeSe flakes after the exfoliation and device fabrication process. (For a detailed discussion, see the Supplemental Material [24]). We infer that the lower T_c^{onset} in the exfoliated flakes can be related to the shift of E_F, which results in the suppression of the contribution from the electron Fermi pockets.

In the gate-voltage-induced high-T_c phase ($V_g = 6.0$ V, $T_c = 45.3$ K), however, the temperature dependence of R_H is strikingly different: R_H is negative, indicating that the dominant carriers are electron type, and decreases gradually with decreasing temperature. We note that at $V_g = 6.0$ V, $R_{xy}(B)$ also exhibits a linearity in the entire temperature range [Supplemental Material, Fig. S5(b) [24]]. The change of the dominant charge carrier at low temperatures from hole type in the as-exfoliated flakes to electron type in the high-T_c phase clearly indicates that applying a positive voltage can introduce electron charge to the surface of the FeSe thin flake. Moreover, the evolution of the R_H-T curves from the as-exfoliated ($V_g = 0$ V) to the electron-doped ($V_g = 6.0$ V) sample mimics the behavior of five-unit-cell FeSe films on a $SrTiO_3$ substrate with the annealing time prolonged from 0 to 36 h [36]. It suggests that the annealing procedure and the gate voltage tuning process play the same role for the enhancement of superconductivity in FeSe thin films. The enhancement of the negative R_H at low temperature at $V_g = 6.0$ V has also been observed for $K_xFe_{2-y}Se_2$ single crystals with $T_c = 32$ K [37] and an optimally doped (Li, Fe)OHFeSe flake with $T_c = 43.4$ K [38]. These similarities hint at a possibly universal underlying physics in these heavily electron doped FeSe superconductors.

The evolution of the Hall signal from hole type to electron type upon applying the gate voltage is summarized in Fig. 3(b). Most intriguingly, an abrupt jump in the value of R_H from positive to negative is observed at $V_g = 4.25$ V, indicating a dramatic modification in the electronic structure in its vicinity induced by charge doping. Here, we note that in a certain voltage range around this jump, the $R_{xy}(B)$ curves exhibit nonlinear behavior as a characteristic of a typical multiband system (Supplemental Material, Fig. S6,

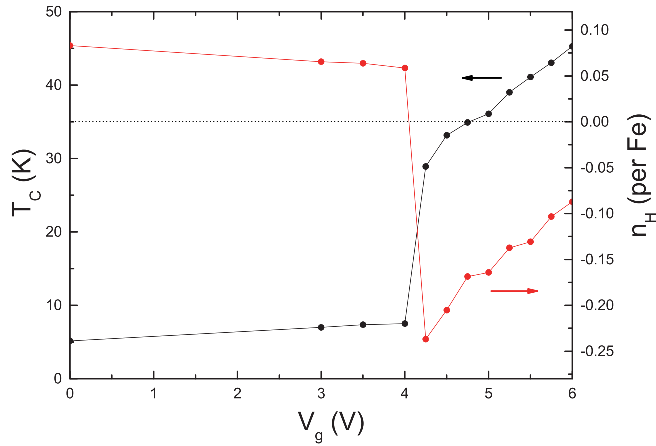

FIG. 4. Superconducting transition temperature and n_H per Fe as a function of gate voltage V_g. T_C shows a clear V_g dependence. A transition from the low-T_c phase to the high-T_c phase occurs at $V_g = 4.25$ V, exactly corresponding to the sudden sign reversal in n_H per Fe.

[24]). For these curves, R_H is also calculated from the slope at the high field end. The most striking feature of the discontinuous jump in R_H is in the coincidence with the appearance of the high-T_c superconducting phase. In Fig. 4, we plot the gate voltage dependence of $T_c^{\rm onset}$ and the effective carrier density (i.e., the Hall number $n_H = 1/eR_H$, at $T = 50$ K) together. Upon applying V_g, n_H initially decreases in accord with an electron doping process, while T_c is also slowly enhanced. At $V_g = 4.25$ V, the high-T_c phase starts to show up, and n_H shows a corresponding sudden sign reversal. The further ramping up of V_g continues to gradually enhance T_c, whereas n_H decreases continuously up to the maximum voltage.

The abnormal behavior observed at $V_g = 4.25$ V is highly likely to be linked to an electronic transition that changes the band structure in FeSe. Previous studies on FeSe confirm it to be a semimetal with both hole and electron pockets around the Fermi level, and the electronic transport properties are dominated by hole carriers [29]. With the doping of electrons into the energy band of FeSe in an EDLT, the effective hole population is suppressed and the dominant carriers change to electrons at a critical voltage close to 4.25 V. The emergence of a high-T_c superconducting transition at the same critical voltage strongly suggests a close connection between the evidently enhanced T_c and the electron-dominated transport properties. We recall that in all of the Fe-chalcogenide systems that host T_c above 30 K, including $A_x\mathrm{Fe}_{2-y}\mathrm{Se}_2$ [1,2], (Li, Fe)OHFeSe [4], and a monolayer FeSe film on SrTiO_3 [5], there are only electron pockets in their electronic structures [6–10,16–20]. A reasonable scenario based on all of the evidence is that the Fermi surface topology in the electron-doped FeSe is significantly modified at a critical band filling, which is usually called the Lifshitz transition [39]. Above the critical electron doping, the hole pockets vanish as the valance bands sink below the Fermi level, and the electronic structures are similar to those of the FeSe-derived high-T_c systems mentioned above. As a result, an appreciably enhanced T_c as high as 48 K is observed. The sudden sign reversal in R_H can serve as an indicator of the Lifshitz transition, yet further experimental evidence is required to unambiguously confirm the existence and details of such a transition.

In summary, gate-voltage-induced high-T_c superconductivity is achieved in FeSe by surface charge accumulation in an EDLT configuration. The optimal critical temperature we observed, $T_c = 48$ K, is so far the highest in the parent material FeSe without any artificial interface. Electron doping thus is proved to be crucial in the optimization of T_c in Fe-chalcogenide systems, and the high T_c above 30 K in these systems is likely to be closely related to the electron pockets as suggested by our Hall data. These observations provide an exceptional example of how electrostatic doping, a clean doping process without any change in crystal structure, can effectively enhance the superconducting transition temperature. In addition, it is should be addressed that 48 K may not be the upper limit of T_c in this electron doping process. It is possible that T_c can reach a higher value with further doping. At the current stage the further increase of doping level is prevented by the possible electrochemical reaction between the sample and the ionic liquid at a high gate voltage ($V_g > 6$ V), which can damage the sample. A more effective method of introducing the carrier into FeSe is required for such an investigation.

This work is supported by the National Natural Science Foundation of China (Grants No. 11190021, No. 11534010 and No. 91422303), the “Strategic Priority Research Program (B)” of the Chinese Academy of Sciences (Grant No. XDB04040100), the National Basic Research Program of China (973 Program, Grant No. 2012CB922002), and the Hefei Science Center CAS (2015SRG-HSC013). Partial work was done at the USTC Center for Micro- and Nanoscale Research and Fabrication at the University of Science and Technology of China, Hefei, Anhui, China.

*Corresponding author.
chenxh@ustc.edu.cn

[1] J. G. Guo, S. F. Jin, G. Wang, S. C. Wang, K. X. Zhu, T. T. Zhou, M. He, and X. L. Chen, Phys. Rev. B **82**, 180520(R) (2010).
[2] A. F. Wang *et al.*, Phys. Rev. B **83**, 060512(R) (2011).
[3] M. Burrard-Lucas *et al.*, Nat. Mater. **12**, 15 (2013).
[4] X. F. Lu *et al.*, Nat. Mater. **14**, 325 (2015).
[5] Q. Y. Wang *et al.*, Chin. Phys. Lett. **29**, 037402 (2012).
[6] X. Liu, L. Zhao, S. L. He, J. F. He, D. F. Liu, D. X. Mou, B. Shen, Y. Hu, J. W. Huang, and X. J. Zhou, J. Phys. Condens. Matter **27**, 183201 (2015).

[7] D. F. Liu *et al.*, Nat. Commun. **3**, 931 (2012).
[8] S. L. He *et al.*, Nat. Mater. **12**, 605 (2013).
[9] S. Y. Tan *et al.*, Nat. Mater. **12**, 634 (2013).
[10] R. Peng *et al.*, Nat. Commun. **5**, 5044 (2014).
[11] J. F. Ge, Z. L. Liu, C. H. Liu, C. L. Cao, D. Qian, Q. K. Xue, Y. Liu, and J. F. Jia, Nat. Mater. **14**, 285 (2015).
[12] Y. Sun, W. H. Zhang, Y. Xing, F. S. Li, Y. F. Zhao, Z. C. Xia, L. L. Wang, X. C. Ma, Q. K. Xue, and J. Wang, Sci. Rep. **4**, 6040 (2014).
[13] F. C. Hsu *et al.*, Proc. Natl. Acad. Sci. U.S.A. **105**, 14262 (2008).
[14] C. L. Song, Y. L. Wang, Y. P. Jiang, Z. Li, L. L. Wang, K. He, X. Chen, X. C. Ma, and Q. K. Xue, Phys. Rev. B **84**, 020503(R) (2011).
[15] Y. Y. Xiang, F. Wang, D. Wang, Q. H. Wang, and D. H. Lee, Phys. Rev. B **86**, 134508 (2012).
[16] X. Liu *et al.*, Nat. Commun. **5**, 5047 (2014).
[17] J. J. Lee *et al.*, Nature (London) **515**, 245 (2014).
[18] Y. Miyata, K. Nakayama, K. Sugawara, T. Sato, and T. Takahashi, Nat. Mater. **14**, 775(2015).
[19] L. Zhao *et al.*, arXiv:1505.06361.
[20] X. H. Niu *et al.*, Phys. Rev. B **92**, 060504(R) (2015).
[21] J. T. Ye, Y. J. Zhang, R. Akashi, M. S. Bahramy, R. Arita, and Y. Iwasa, Science **338**, 1193 (2012).
[22] J. T. Ye, S. Inoue, K. Kobayashi, Y. Kasahara, H. T. Yuan, H. Shimotani, and Y. Iwasa, Nat. Mater. **9**, 125 (2010).
[23] H. T. Yuan, H. Shimotani, A. Tsukazaki, A. Ohtomo, M. Kawasaki, and Y. Iwasa, Adv. Funct. Mater. **19**, 1046 (2009).
[24] See Supplemental Material at http://link.aps.org/supplemental/10.1103/PhysRevLett.116.077002, which includes Refs. [25–34], for details of device fabrication and additional data for the gate-tuned transport properties.
[25] A. E. Böhmer, F. Hardy, F. Eilers, D. Ernst, P. Adelmann, P. Schweiss, T. Wolf, and C. Meingast, Phys. Rev. B **87**, 180505(R) (2013).
[26] S. I. Vedeneev, B. A. Piot, D. K. Maude, and A. V. Sadakov, Phys. Rev. B **87**, 134512 (2013).
[27] S. Knöner, D. Zielke, S. Köhler, B. Wolf, Th. Wolf, L. Wang, A. Böhmer, C. Meingast, and M. Lang, Phys. Rev. B **91**, 174510 (2015).
[28] H. C. Lei, D. Graf, R. W. Hu, H. Ryu, E. S. Choi, S. W. Tozer, and C. Petrovic, Phys. Rev. B **85**, 094515 (2012).
[29] M. D. Watson *et al.*, Phys. Rev. Lett. **115**, 027006 (2015).
[30] T. P. Ying, X. L. Chen, G. Wang, S. F. Jin, T. T. Zhou, X. F. Lai, H. Zhang, and W. Y. Wang, Sci. Rep. **2**, 426 (2012).
[31] A. Krzton-Maziopa, E. V. Pomjakushina, V. Y. Pomjakushin, F. von Rohr, A. Schilling, and K. Conder, J. Phys. Condens. Matter **24**, 382202 (2012).
[32] X. Dong, K. Jin, D. Yuan, H. Zhou, J. Yuan, Y. Huang, W. Hua, J. Sun, P. Zheng, W. Hu, Y. Mao, M. Ma, G. Zhang, F. Zhou, and Z. Zhao, Phys. Rev. B **92**, 064515 (2015).
[33] K. K. Huynh, Y. Tanabe, T. Urata, H. Oguro, S. Heguri, K. Watanabe, and K. Tanigaki, Phys. Rev. B **90**, 144516 (2014).
[34] T. Terashima *et al.*, Phys. Rev. B **90**, 144517 (2014).
[35] K. Ueno, S. Nakamura, H. Shimotani, H. T. Yuan, N. Kimura, T. Nojima, H. Aoki, Y. Iwasa, and M. Kawasaki, Nat. Nanotechnol. **6**, 408 (2011).
[36] Q. Wang, W. Zhang, Z. Zhang, Y. Sun, Y. Xing, Y. Wang, L. Wang, X. Ma, Q.-K. Xue, and J. Wang, 2D Mater. **2**, 044012 (2015).
[37] X. X. Ding, Y. M. Pan, H. Yang, and H. H. Wen, Phys. Rev. B **89**, 224515 (2014).
[38] B. Lei, Z. J. Xiang, X. F. Lu, N. Z. Wang, J. R. Chang, C. Shang, X. G. Luo, T. Wu, Z. Sun, and X. H. Chen, arXiv:1503.02457.
[39] I. M. Lifshitz, Sov. Phys. JETP **11**, 1130 (1960).